

## An Amino Acid Grafted Graphene Oxide as Promising Material in Poly(urea-formaldehyde)-Epoxy Microcapsules for Enhancing the Interfacial Adhesion of Epoxy Coatings

D. PRIYANKA\*<sup>ORCID</sup> and D. NALINI<sup>ORCID</sup>

Department of Chemistry, PSGR Krishnammal College for Women, Coimbatore-641004, India

\*Corresponding author: E-mail: [nalini@psgrkcw.ac.in](mailto:nalini@psgrkcw.ac.in); [priyankapsgrkcw@gmail.com](mailto:priyankapsgrkcw@gmail.com)

Received: 27 October 2022;

Accepted: 31 January 2023;

Published online: 27 February 2023;

AJC-21159

Novel microencapsulated materials with superior anti-corrosion properties and improved adhesive strength on the metal substrate were produced by emulsion polymerization and characterized successfully. Initially, serine grafted graphene oxide was prepared and characterized through various sophisticated techniques. Then, MC-GO/epoxy and MC-GO-Ser were individually impregnated into the epoxy system and applied on the mild steel substrates. Corrosion tests were performed to evaluate the non-corrosive nature of MC-GO/epoxy and MC-GO-Ser/epoxy samples. After 7 days of exposure in saline media, MC-GO-Ser microcapsules demonstrated 80.6 % protective efficiency. Furthermore, the peel strength of 2.90 N revealed that the coating loaded with MC-GO-Ser microcapsules had improved adherence to the mild steel surface. Results of urea-formaldehyde GO-Ser microcapsules showed better corrosion protection and greater adhesive strength, which is probably because of the exceptional barrier action of microcapsules against the incursion of corrosion solution onto the mild steel surface.

**Keywords:** Epoxy coatings, Urea-formaldehyde, Microencapsulation, Corrosion-resistivity, Adhesion.

### INTRODUCTION

Even though rust is a serious issue for maritime equipments, marine strategies are becoming increasingly vital to the prosperity of any nation. These kinds of equipment are utilized to last a long time in harsh environments [1,2]. The most practical and efficient method of protecting the mild steel surface against corrosion species' attack is to apply coatings. Epoxy coatings draw significant attention among the many coating techniques because they continue to offer protection even under challenging conditions. When the organic coatings are fabricated on the surface of metal substrates, the corrosion rate is declined through three main mechanisms *viz.* protective barrier, sacrificial and inhibition [3-6]. The nature, composition and percentage of the fillers available determine the properties of organic coatings, which are typically fillers disseminated in the binding medium. Generally, organic coatings are manifested by the nature, composition and proportion of the fillers available in them. Unfortunately, the corrosion agents tend to penetrate and reach the coating-steel interface, through the microscopic pores. This leads to an increase in adhesion loss and induces the coating to blister [7-11].

Nowadays, protective coatings applied to steel substrates benefit significantly from the use of microcapsules made up of diverse active agents. Microcapsules offer the opportunity to release encapsulated active inhibitors to minimize the mechanisms of corrosion occurring on the mild steel surface [12]. Organic-based corrosion inhibitors have not been thoroughly explored, despite the fact that microcapsules containing a variety of substances are well recognized to be utilized as anti-corrosion agents. Many workers proposed several innovative strategies to improve barrier activity by improving the coating's adherence to substrates by using anti-corrosive additives/fillers [13]. Epoxy resin has been filled with a variety of particles, including SiO<sub>2</sub> [3-5], TiO<sub>2</sub> [6,7], Cr<sub>2</sub>O<sub>3</sub> [14], Al<sub>2</sub>O<sub>3</sub> [15] and Fe<sub>2</sub>O<sub>3</sub> [4]. There are different filler types that differ particularly in shape, such as spherical, rod-like and sheet-like structures [16]. Sheet-like structures are known to offer better barrier characteristics than the other structures [17].

The main objective of this work is to build up a novel technique in favour of improving the epoxy coating's ability to withstand corrosion and the strength of its adhesive bond. It was thought that chemically grafting graphene oxide (GO)

sheets with the amino acid L-serine would strengthen the binding between the neat epoxy system and the metal surface. Accordingly, during the dehydration reaction, GO sheets were developed and grafted with serine. The EDS, SEM and FT-IR analyses were used to characterize the grafted GO sheets. *In situ* polymerization was used to develop urea-formaldehyde microcapsules embedded in the GO-Ser sheets. The obtained microcapsules in an epoxy matrix were characterized in order to reveal the impact on anti-corrosion properties and adhesive strength.

### EXPERIMENTAL

Without using any advanced purification techniques, all chemicals utilized for the grafting of graphene oxide and the preparation of microcapsules were acquired from Sigma-Aldrich, USA. For coating purposes, mild steel specimens measuring 50 mm × 10 mm × 0.05 mm were employed. The percentage composition of the mild steel sample is shown in Table-1. The polyamide (hardener) and an epoxy resin having epoxy value, solid nature and density of 0.1367-0.1645, 73-76% and, 0.97 g/cm<sup>3</sup>, respectively were procured from Covai Seenu & Company, India. The steel substrates were abraded with 2000 and 2400 grade SiC sheets prior to coating. The mild steel substrates were then cleaned with deionized water and acetone.

**Preparation of GO:** Hummers' method was utilized for the synthesis of GO sheets as reported earlier [18-21].

**Preparation of serine grafted GO (GO-Ser):** The synthesized GO was added in 60 mL of distilled water and subjected to ultrasonication for 3 h. This solution was treated with 0.6 g of serine and 1 mL of conc. H<sub>2</sub>SO<sub>4</sub> and stirred at 80 °C for 5 h. Then, the mixture was centrifuged at 3000 rpm for 10 min. The residue was purified thoroughly by washing with ethanol. At last, graphene oxide sheets grafted with serine were filtered and dried. The schematic description of the preparation of GO-Ser sheets is shown in Fig. 1.

**Fabrication of MC-GO/GO-Ser microcapsules on mild steel substrates:** Formaldehyde and urea were used to synthesize urea-formaldehyde microcapsules that contained GO/GO-Ser. In 60 mL of deionized water, urea (4.8 g), ammonium chloride (0.2 g) and resorcinol (0.2 g) were dispersed. To the above solution, 10 mL of resorcinol was added to build the shell for microcapsule [22]. Deionized water (10 mL) and GO/GO-Ser sheets (0.05 g) were blended together with the help of an ultrasonicator for 10 min. Following that the GO/GO-Ser suspensions were introduced one at a time to the microcapsule solution. In order to mix the microcapsule solution, 20 mL of epoxy resin was added dropwise after the pH was corrected to 3.5 with HCl solution. This solution was stirred for 15 min at 800 rpm to stabilize followed by the addition of 3.0 mL of HCHO while stirring. The temperature was raised to 70 °C and stirring was maintained for about 4 h. Then, the mixture was filtered and cleaned with acetone, deionized and dried. Wet transfer was used to transfer the dried microcapsules that had been sonicated in DMF to the epoxy matrix. The mixture was placed in an oven for 48 h at 80 °C to remove DMF. Later, GO and GO-Ser encapsulated microcapsules were reacted with hardener (2:1, w/w) and fabricated on the steel surface that had been thoroughly cleaned (sandblasted with sandpapers and then degreased with acetone). The coated samples were dried out for 1 day before being heated for approximately 6 h at 120 °C to cure them. The dry thickness of the steel samples was ~1 mm.

**Characterization:** FT-IR studies in the range 4000-400 cm<sup>-1</sup> using SHIMADZU IRAffinity-1S spectrometer on KBr pellet were carried out to examine the extent of bonding between GO, GO-Ser sheets and epoxy resin, and also to confirm the formation of microcapsules. The FE-SEM and EDX analyses were done to study the surface morphology and the chemical composition of neat GO/GO-Ser and GO/GO-Ser enclosed microcapsules by MIRA TESCAN model FE-SEM analyzer.

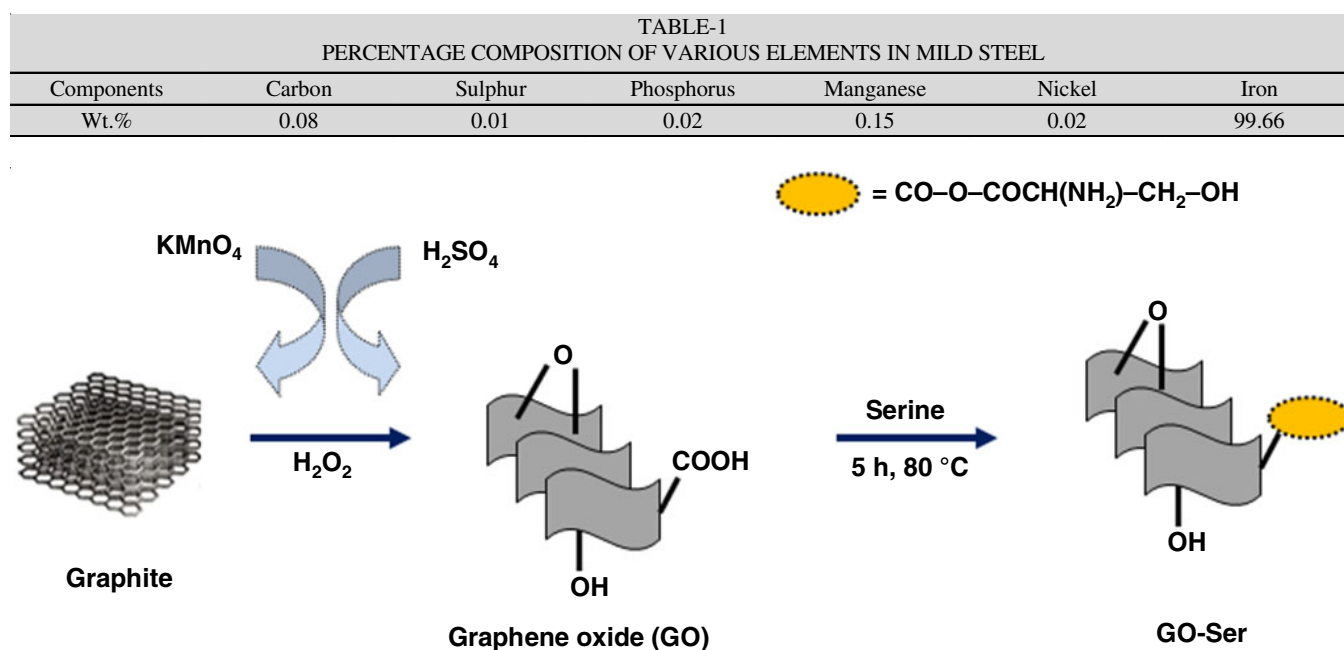


Fig. 1. Schematic diagram describing the preparation of GO-Ser

The contact angle was calculated so as to assess the surface wettability qualities of coated samples. At room temperature, electrochemical impedance and the potentiodynamic polarization studies were accustomed to observe the impact of GO and GO-Ser on the anticorrosion properties. According to ASTM G-72 [23], the analyses were performed in saline media at various exposure periods. The three-electrode setup used for the EIS studies has an area of approximately  $1 \text{ cm}^2$  and a sinusoidal amplitude of 10 mV. Utilizing the software NOVA Auto lab (version 6), the measurements were made throughout. Thermal studies were done to study the thermal characteristics of the prepared microcapsules (Perkin-Elmer, TGA 400). In this experiment, the percentage loss of mass was calculated within the temperature range of 0-500 °C in nitrogen atmosphere using 5-6 mg of sample.

To study the wettability characteristics of neat epoxy and composites containing GO and GO-Ser, contact angle measurements were used. For this, a contact angle measurement device called OCA 20 was used. The effect of microcapsules on the neat epoxy coatings was investigated using a salt spray test in accordance with international standard ASTM B117. An X-mark with dimensions of 1 mm in width and 2.5 cm in length was cut out with a penknife and placed in the salt spray chamber at a 45° angle. Additionally, coated substrates were constantly exposed for roughly 12 days to a 5 wt.% NaCl solution with a pH range of 6.5 to 7.2. Condensate was accumulated in the cabinet at a rate of 1.0 to 2.0 mL/h.

A peel-off adhesion test was performed using the ASTM D 4551 method to estimate the ability of coating to stick to steel surfaces. The coated surface was covered with polyimide Kapton tape, which was then peeled off at 90° angle with a constant force. At a rate of 20 mm/min, the surface coating of the mild steel was removed.

## RESULTS AND DISCUSSION

### Characterization of GO and GO-Ser

**FT-IR studies:** The FT-IR spectrum (Fig. 2) showed that serine had successfully been grafted onto the GO surface. The widening of the GO spectra at  $3558 \text{ cm}^{-1}$  was caused by the

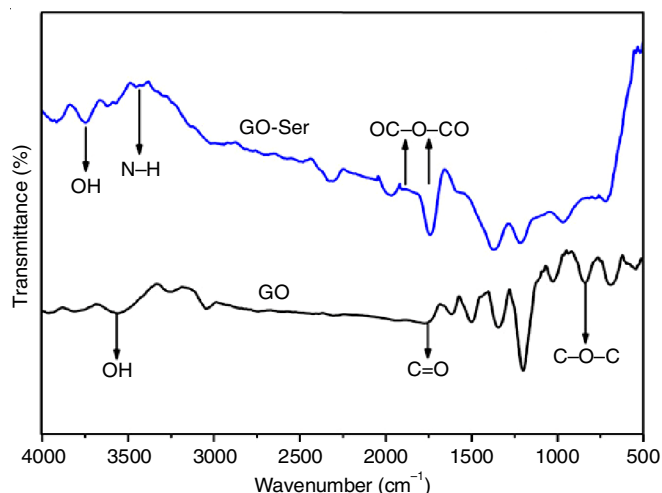


Fig. 2. IR Spectra of GO and GO-Ser

presence of hydroxyl moiety. The stretchings of carboxylic acid (C-O, C=O and -OH) correspond to the frequency bands at 1347, 1773 and  $3046 \text{ cm}^{-1}$ , respectively. Two break up pointed bands observed at 817 and  $1226 \text{ cm}^{-1}$  were attributed to C-O-C stretchings. These absorption peaks indicated that the occurrence of oxygenous moieties on GO sheets, which coincides well with previously reported in the literature [24]. After the grafting process, new peaks observed at 1845.78 and  $1741.74 \text{ cm}^{-1}$  were assigned to the anhydride group. This clearly showed the condensation reaction among the carboxyl groups of both serine and GO sheets. The bands at 3423.79, 1217.08 and  $3612.19 \text{ cm}^{-1}$  confirmed the occurrence of -N-H, -C-N and -OH bonds of serine moiety in GO-Ser sheets, respectively. After 2 days of suspension, the GO and GO-Ser sheets retain their stability which was attributed to the presence of hydrophilic groups such as hydroxyl and carbonyl moieties on their surface.

**FE-SEM studies:** By using FE-SEM images, the impact of grafting of an amino acid on the surface of GO sheets was examined. Fig. 3a displayed the uneven folding and wrinkled of GO sheets. This demonstrated unequivocally that the oxidation process of graphite involved exfoliation. This might be the result of graphite being distorted when oxygenous groups

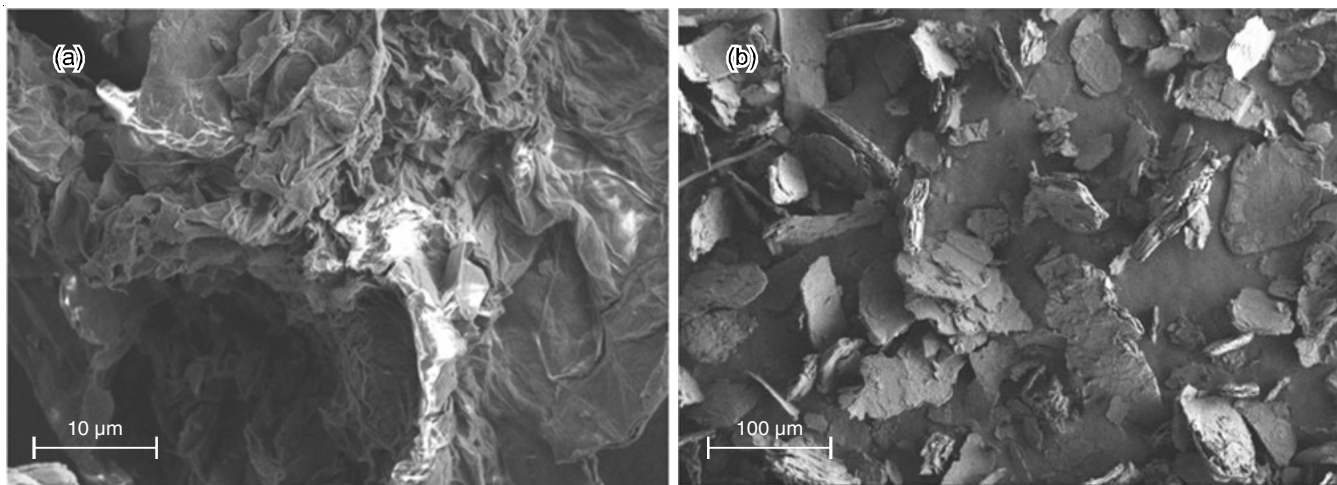


Fig. 3. FE-SEM images of (a) GO and (b) GO-Ser

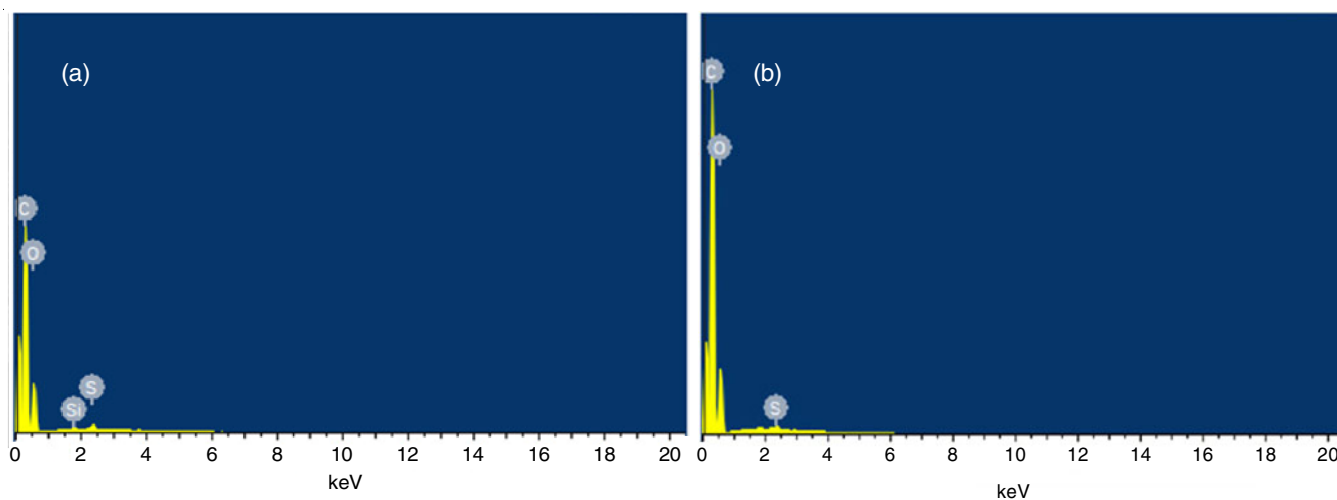


Fig. 4. EDX images of (a) GO and (b) GO-Ser

are added to it in order to create graphene oxide [25]. Following the grafting procedure, the restacking procedure has deformed the shattered structures of GO sheets into layered structures (Fig. 3b). These results demonstrated unambiguously that the surface morphology of GO sheets is greatly influenced by the grafting process.

**EDX studies:** EDX image of GO sheets in Fig. 4a showed peaks related to C (70.8%), O (28.93%), Si (0.05%) and S (0.22%). Upon grafting, GO-Ser sheets (Fig. 4b) showed a meager increase in carbon percentage and a decrease in oxygen percentage when compared neat GO. The C:O ratio of GO and GO-Ser was found to be 1.38: 0.60 and 1.44: 0.55, respectively. This successfully evidenced the grafting of GO sheets by serine moiety.

#### Characterization of MC-GO/GO-Ser microcapsules

**FT-IR studies:** Fig. 5 illustrates the FT-IR spectra of microcapsules MC-GO and MC-GO-Ser. The N-H, C=O and N-H stretchings of urea was identified as the characteristic frequencies at 3339, 1607 and 1526  $\text{cm}^{-1}$ , respectively in the shell of

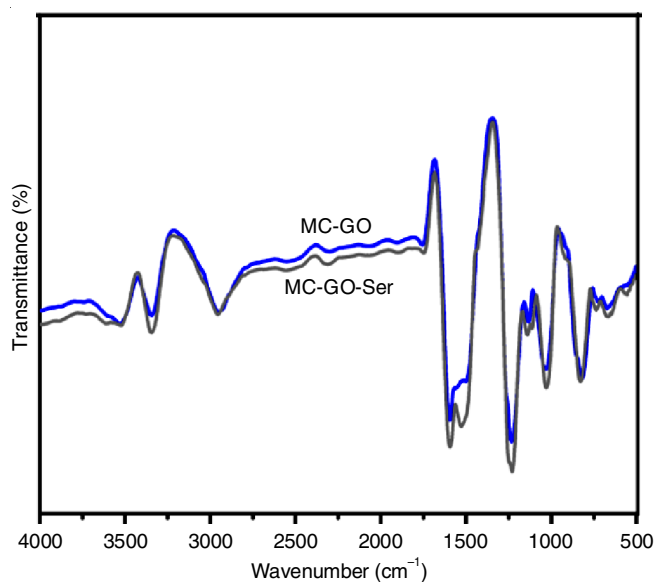


Fig. 5. FT-IR spectra of MC-GO and MC-GO-Ser microcapsules

MC-GO and MC-GO-Ser. Deposition of an epoxy resin on the core was observed at 1030 and 2935  $\text{cm}^{-1}$  which accredited to the occurrence of  $sp^3$  C-H stretching of methyl groups. These bands showed the successful introduction of GO and GO-Ser within urea-formaldehyde shell. Peaks corresponding to GO could not be seen due to the overlapping of bands [22].

**FE-SEM studies:** Fig. 6 depicts the surface shape of microcapsules as determined by FE-SEM analyses. The majority of the microcapsules were found to be sphere-shaped, which assured the capsule storage capacity and a noticeable microcapsule distribution in the neat epoxy system. The surface of the microcapsules was observed to be rough due to the protruding form of the capsule shell. The size of the microcapsules would be more controlled by the range of urea-formaldehyde deposited on the core.

**Thermal studies:** Fig. 7 displays the TGA and DSC thermograms of the MC-GO and MC-GO-Ser microcapsules. The fact that the initial degradation was observed between 270 and 310  $^{\circ}\text{C}$  and was attributed to the DSC (inflection point) at 272  $^{\circ}\text{C}$  demonstrates that the synthesized MC-GO and MC-GO-Ser microcapsules are stable up to 270  $^{\circ}\text{C}$ . This deterioration was attributed to the thermally persuaded breakdown of the capsule wall material; nevertheless, the processes like as cross-linking and depolymerization may occur above this temperature. Additionally, the two-step degradation demonstrated the presence of GO in the poly(urea-formaldehyde) core. Formaldehyde deterioration from the capsule shell and core material was observed between 310 and 460  $^{\circ}\text{C}$ , which corresponds to the DSC (inflection point) at 370  $^{\circ}\text{C}$ . Due to the occurrence of core material, weight loss was observed above 470  $^{\circ}\text{C}$ . This confirmed that the capsule wall has enclosed GO and GO-Ser sheets. As a result of the higher concentration of GO and its derivative, produced microcapsules exhibit a wide range of weight loss % during the second stage.

#### Evaluation of MC-GO/GO-Ser/epoxy composites against corrosion

**Polarization studies:** Polarization analysis was done to estimate the anticorrosion efficiency of MC-GO and MC-GO-Ser in an epoxy matrix coated on steel samples immersed in

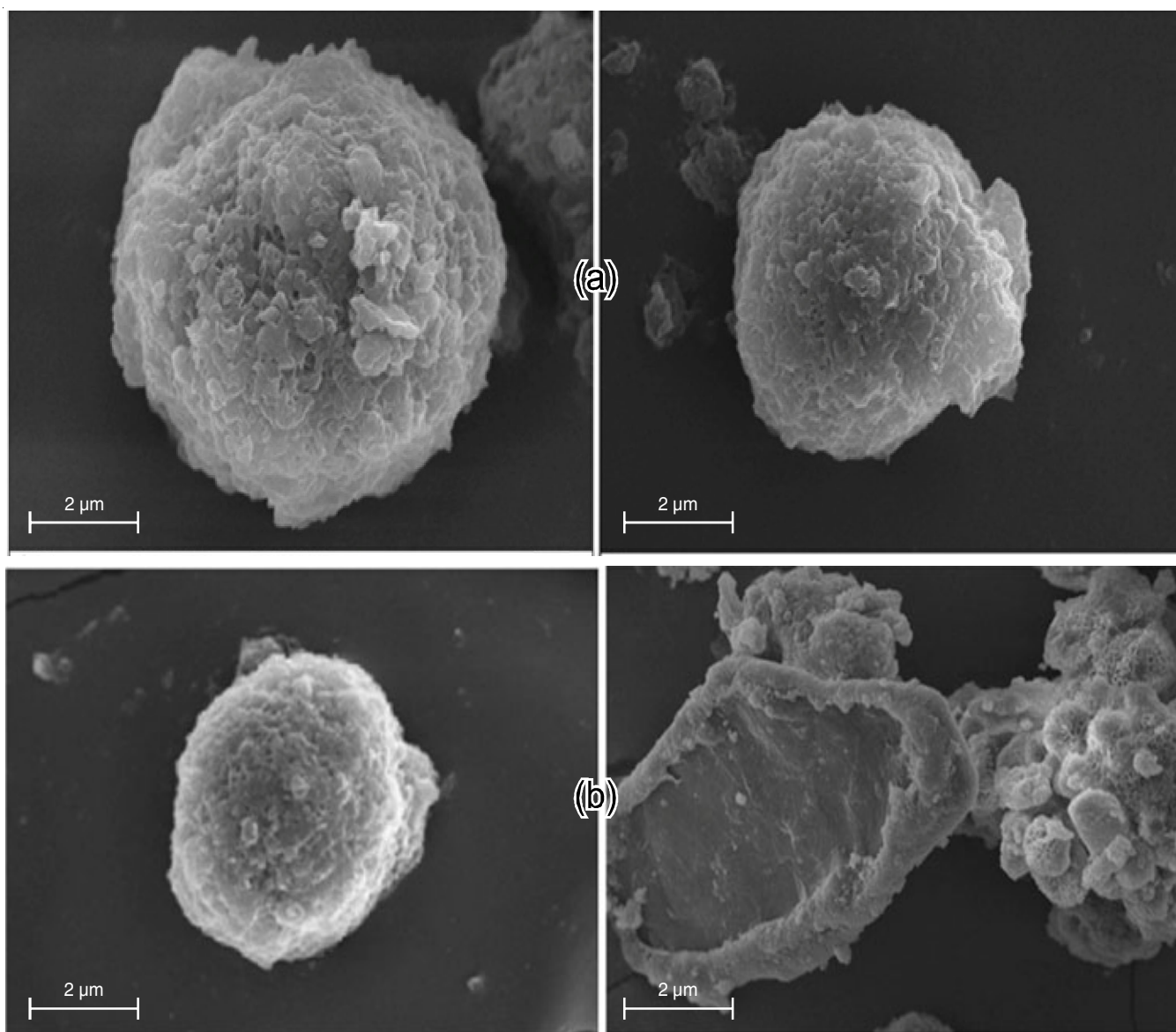


Fig. 6. FE-SEM photographs of (a) MC-GO (b) MC-GO-Ser

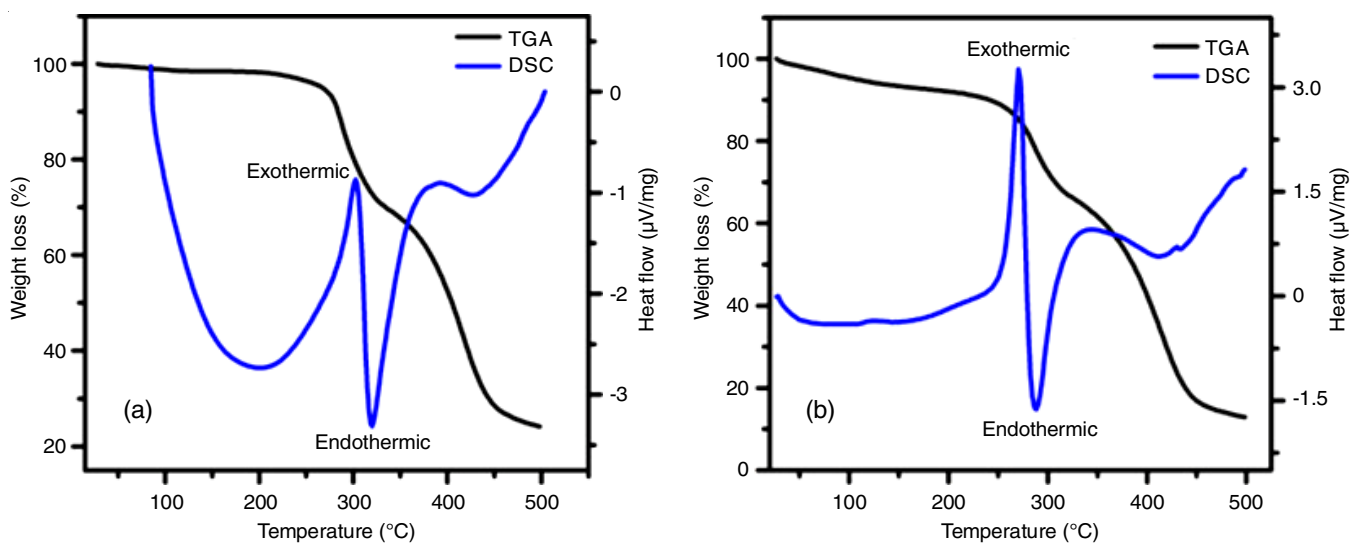


Fig. 7. TGA and DSC plots of (a) MC-GO (b) MC-GO-Ser

3.5% NaCl solution after 7 days. The potentiodynamic plots acquired at 298 K for neat epoxy, MC-GO/epoxy and MC-GO-Ser/epoxy coated substrates are shown in Fig. 8. The outcome of the extrapolation of Tafel curves is summarized in Table-2. It can be seen from Fig. 8 that anodic and cathodic branches of the polarization curve of MC-GO-Ser/epoxy sample show the depression to lower current density values. The results revealed that  $E_{\text{corr}}$  measurements of MC-GO-Ser/epoxy (-0.5102 V) reallocate towards the positive side from the potential of neat epoxy sample, which is around 203 mV after 7 days of exposure in 3.5% NaCl solution. While MC-GO/epoxy coating shows the positive shift of about 178 mV from  $E_{\text{corr}}$  value of the neat steel sample (-0.5329 V). The MC-GO/epoxy and MC-GO-Ser/epoxy samples showed a pronounced decrease in  $i_{\text{corr}}$  value notably when related to neat epoxy coated samples. In addition, the polarization resistance and cathodic Tafel slope of MC-GO/epoxy and MC-GO-Ser/epoxy sample has been improved suggesting the improved anti-corrosion process. The corrosion protection percentage of steel substrates was calculated via the following eqn. (1) [10]:

$$P_{\text{EF}}(\%) = \frac{i_{\text{corr}}(\text{uncoated}) - i_{\text{corr}}(\text{coated})}{i_{\text{corr}}(\text{uncoated})} \times 100 \quad (1)$$

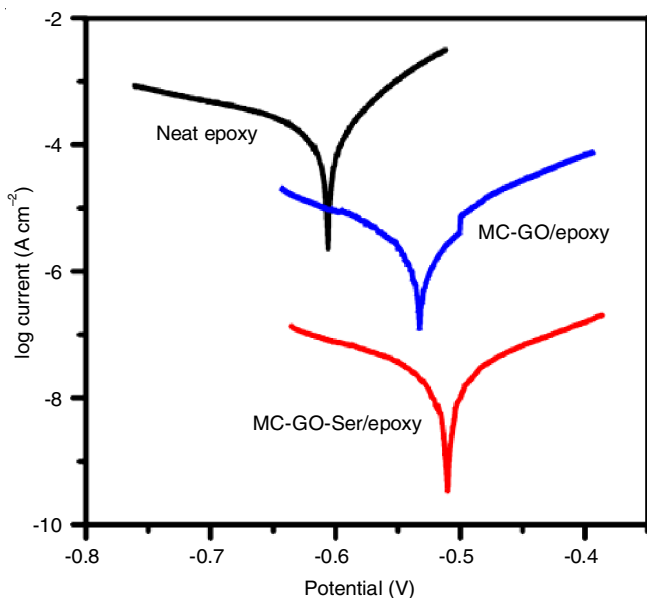


Fig. 8. Polarization curves of epoxy coated samples after 7 d exposure in corrosion solution

The protection efficiency of MC-GO-Ser/epoxy coated sample was found to be 80.6%.

**OCP Measurements:** To evidence, the consequence of additives in an epoxy system, OCP (vs. SCE) measurements was done for the epoxy-coated steel substrates in 3.5% NaCl

solution. Fig. 9 shows OCP values of epoxy coated samples at various immersion periods. Table-3 shows that the OCP measurements of all the samples decreases with an increase in exposure times [26], which is due to the intrusion of electrolytes into the film. However, the epoxy sample containing MC-GO-Ser sheets records more positive OCP values in comparison with other samples. This implies that the additives added into the epoxy matrix have improved the potential barrier between the coating/substrate interface by blocking the micro-cavities present in the neat epoxy matrix.

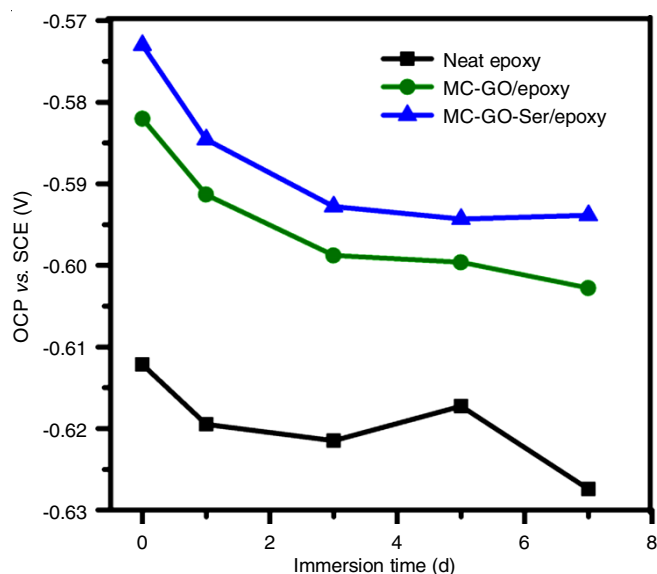


Fig. 9. OCP curves of neat EP, GO/EP and GO-Ser/EP coatings after 7 d

**EIS studies:** EIS studies were done to study the effect of the inoculation of MC-GO and MC-GO-Ser into urea-formaldehyde microcapsules. Fig. 10 shows Nyquist plots of MC-GO/epoxy and MC-GO-Ser/epoxy coated systems after various immersion periods over 7 days in 3.5% NaCl solution. The logarithm of impedance ( $\log |Z|_{100 \text{ mHz}}$ ) and phase angle ( $-\theta_{100 \text{ kHz}}$ ) values are displayed in Table-3. The findings indicate that coating resistance ( $R_c$  value) decreases with exposure duration from 1 h to 7 days, indicating a reduction in the ingress of corrosive agents onto the coating surface. It is clear that the total resistance ( $R_t$ ) values of samples containing microcapsules significantly rise, demonstrating the better anti-corrosion ability (Fig. 11).

**Salt spray test:** The visual images of the epoxy systems containing MC-GO and MC-GO-Ser exposed to 5.0% NaCl solution for different exposure periods (7 days and 14 days) in salt spray chamber are depicted in Fig. 12. Images show the accretion of corrosive deposits and blisters around engrave on the unmodified epoxy coated specimen after 144 h subject to the corrosion electrolyte. On increasing the exposure period

TABLE-2  
POTENTIODYNAMIC PARAMETERS OF EPOXY COATED SAMPLES AFTER 7 d

Samples	$E_{\text{corr}}$ (V)	$i_{\text{corr}}$ ( $\mu\text{A}/\text{cm}^2$ )	$\beta_a$ (V/dec)	$\beta_c$ (V/dec)	$R_p$ ( $\text{k}\Omega \text{ cm}^2$ )	Thickness ( $\mu\text{m}$ )	$P_{\text{EF}}$ (%)
Neat EP	-0.7115	9.8	0.2925	0.0801	0.114	55	–
MC-GO/EP	-0.5329	3.6	0.1355	0.2016	8.120	55	63.3
MC-GO-Ser/EP	-0.5102	2.3	0.0998	0.2231	11.794	55	80.6

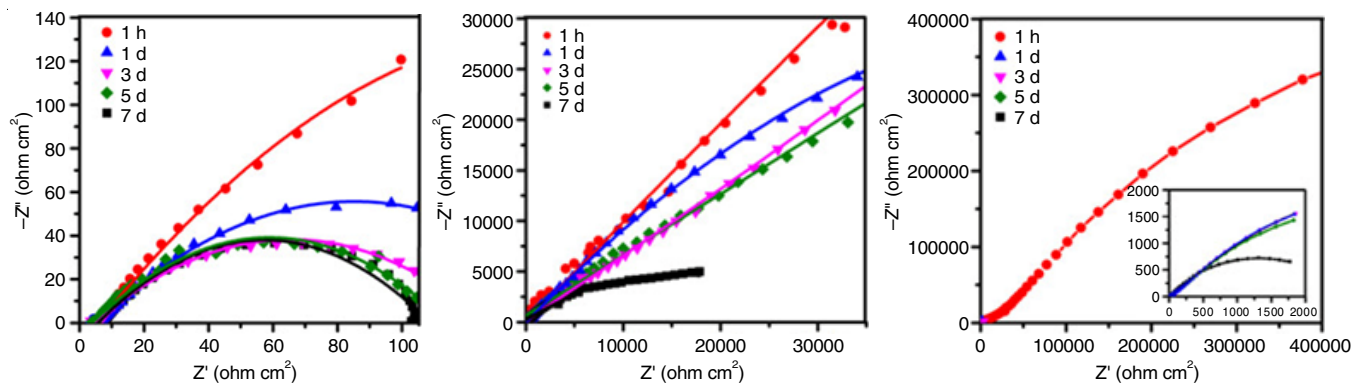


Fig. 10. Nyquist plots of neat EP, MC-GO/EP and MC-GO-Ser/EP coated samples

TABLE-3  
ELECTROCHEMICAL INDICES ACQUIRED FOR EPOXY (EP) COATED SAMPLES IN DIFFERENT IMMERSION PERIODS

Sample	Immersion time	$R_{ct}$ (ohm $cm^2$ )	$R_c$ (ohm $cm^2$ )	$R_t$ (ohm $cm^2$ )	$\log  Z _{100\text{ mHz}}$ (ohm $cm^2$ )	$-\theta_{100\text{ kHz}}$ ( $^\circ$ )	OCP vs. SCE (V)
Neat EP	1 h	1680	85.4	1856.4	3.38	20.03	-0.6112
Neat EP	1 d	1680	117	1877	3.37	16.87	-0.6185
Neat EP	3 d	1420	94.2	1603.2	3.34	17.99	-0.6205
Neat EP	5 d	715	82.6	886.6	3.07	15.61	-0.6163
Neat EP	7 d	577	66.3	732.3	2.89	14.30	-0.6264
MC-GO/EP	1 h	4190	4410	8610	3.68	31.46	-0.5810
MC-GO/EP	1 d	3210	3840	7320	3.59	43.39	-0.5904
MC-GO/EP	3 d	2110	2490	4810	3.37	49.22	-0.5978
MC-GO/EP	5 d	2020	1871	4081	3.35	44.74	-0.5986
MC-GO/EP	7 d	1776	1290	3056	3.27	42.41	-0.6018
MC-GO-Ser/EP	1 h	11700	5478	17178	5.80	49.77	-0.5730
MC-GO-Ser/EP	1 d	10504	4390	14894	5.01	54.71	-0.5846
MC-GO-Ser/EP	3 d	7675	5674	13349	4.82	28.42	-0.5928
MC-GO-Ser/EP	5 d	7848	3489	11337	4.67	62.40	-0.5843
MC-GO-Ser/EP	7 d	7235	2675	9910	4.26	64.11	-0.5939

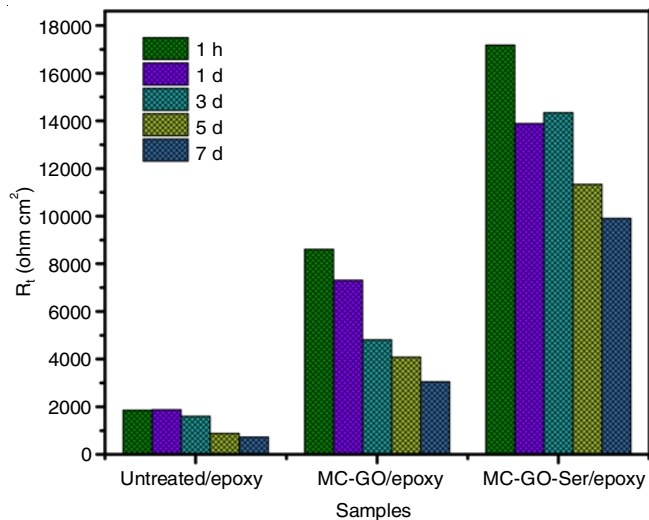


Fig. 11. Total resistance ( $R_t$ ) for neat, MC-GO/EP and MC-GO-Ser/EP steel samples

to 300 h, more and more blisters were accumulated on the artificially inscribed. This might be attributed to the ingress of corrosive products into the interface between the coating and substrate surface through X-mark. There is a reduction in the deposition of corrosive particles and blisters around the scribes after the inclusion of MC-GO and MC-GO-Ser into an epoxy system.

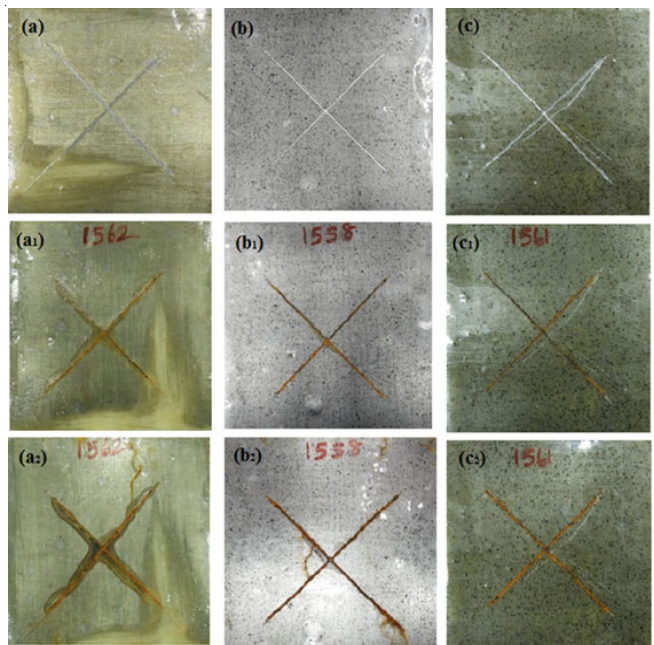


Fig. 12. Salt spray test results of (a) neat EP (b) MC-GO/EP (c) MC-GO-Ser/EP after 7 d and 14 d

**Contact angle:** Contact angle values were used to examine the wettability of neat epoxy and urea-formaldehyde/epoxy

composites comprising MC-GO and MC-GO-Ser. During the measurements, a drop of deionized water was placed on the sample surface and after 10 s, the contact angle between sample and droplet was measured with the help of Canon type camera. From the contact angle ( $\theta$ ) shown in Fig. 13,  $W_a$  (surface free energy) was derived by Neumann equations [27]. The results (Table-4) revealed that the sample with the higher contact angle has the lower value of surface free energy which was related to neat epoxy sample. The samples coated with epoxy composites containing MC-GO and MC-GO-Ser caused surface free energy ( $W_a$ ) to decrease and the contact angle to increase, from 68.2° to 74.2° and 82.4°, respectively.

Metal substrates	$\theta$ (°)	$W_a$ (mJ/m <sup>2</sup> )
Neat EP	68.2	98.7
MC-GO/EP	74.2	91.6
MC-GO-Ser/EP	82.4	81.5

**Mechanical peel-off test:** The quality of the epoxy film relies on the adhesion to the steel surface. Hence, peel-off test was conducted to evidence the adhesive strength of an epoxy system. The load-displacement plots of the coated samples are displayed in Fig. 14. At the beginning of peeling process, the load increases with an increase in displacement. Once the peeling process gets started, a constant plateau follows the steady-state of the load. In the steady-state level, the fluctuation of load (N) occurs, which is the direct reflection of the stability and adhesive strength of the coating along its length [28]. The

mean load at the plateau regions is consistent with peel strength, having a unit of Newton. It is obvious from Table-5 that MC-GO-Ser/epoxy coating has maximum peel strength of 2.90 N and a standard deviation of 0.55 N. This recommended that as a result of strong cohesion, there subsist adhesive interactions between the additive and epoxy matrix [24]. This shows that microcapsule with GO-Ser sheets has good adhesion strength on the steel substrate.

Coated substrates	Peel strength (N)
Neat epoxy	0.86
MC-GO/epoxy	2.34
MC-GO-Ser/epoxy	2.90

**Mechanism:** Fig. 15 depicts poly(urea-formaldehyde) microcapsules filled with GO and GO-Ser sheets acted as core materials. The synthesis of microcapsules takes two steps: (i) basic methylation step where urea reacts with formaldehyde to form methylol ureas and (ii) condensation step involving the formation of urea-formaldehyde dimers, trimers and oligomers of methylol ureas. During the process, NH<sub>4</sub>Cl was added, which improves the strength and sealing performance of the microcapsules. As a result of the active materials formed by the reaction of NH<sub>4</sub>Cl and hydroxymethylol urea, the rough surface of microcapsule can be explained by the precipitation of urea-formaldehyde particles from the emulsion to an inhibitor-water interface [29]:

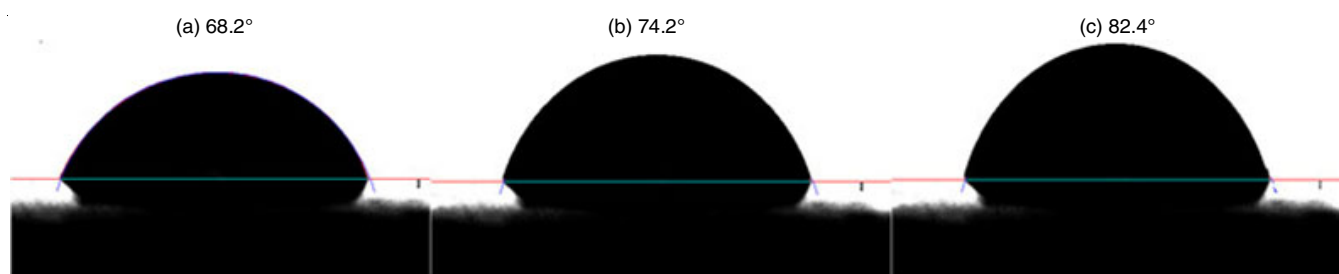


Fig. 13. Contact angle values of (a) neat EP, (b) MC-GO/EP and (c) MC-GO-Ser/EP coatings

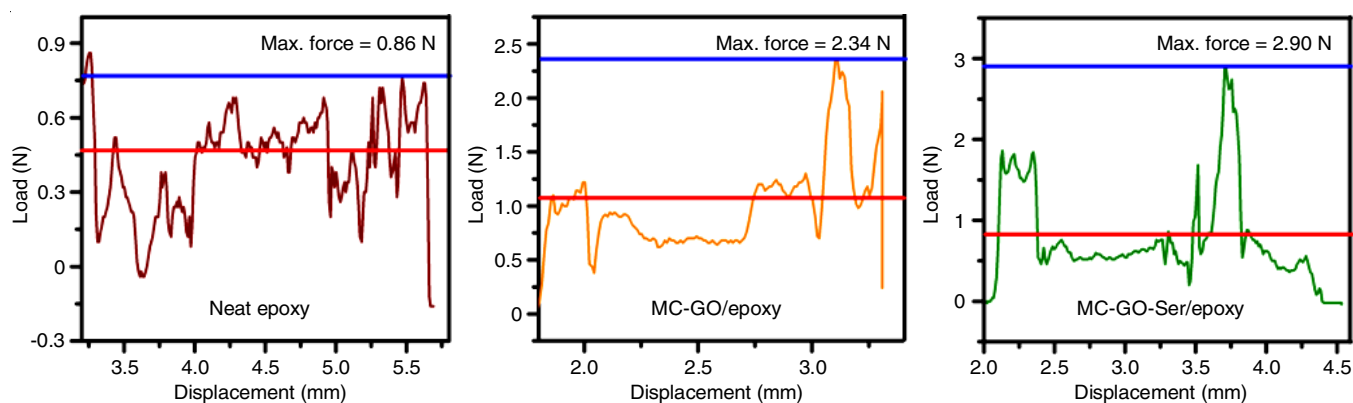


Fig. 14. Load-displacement plots of the steel samples

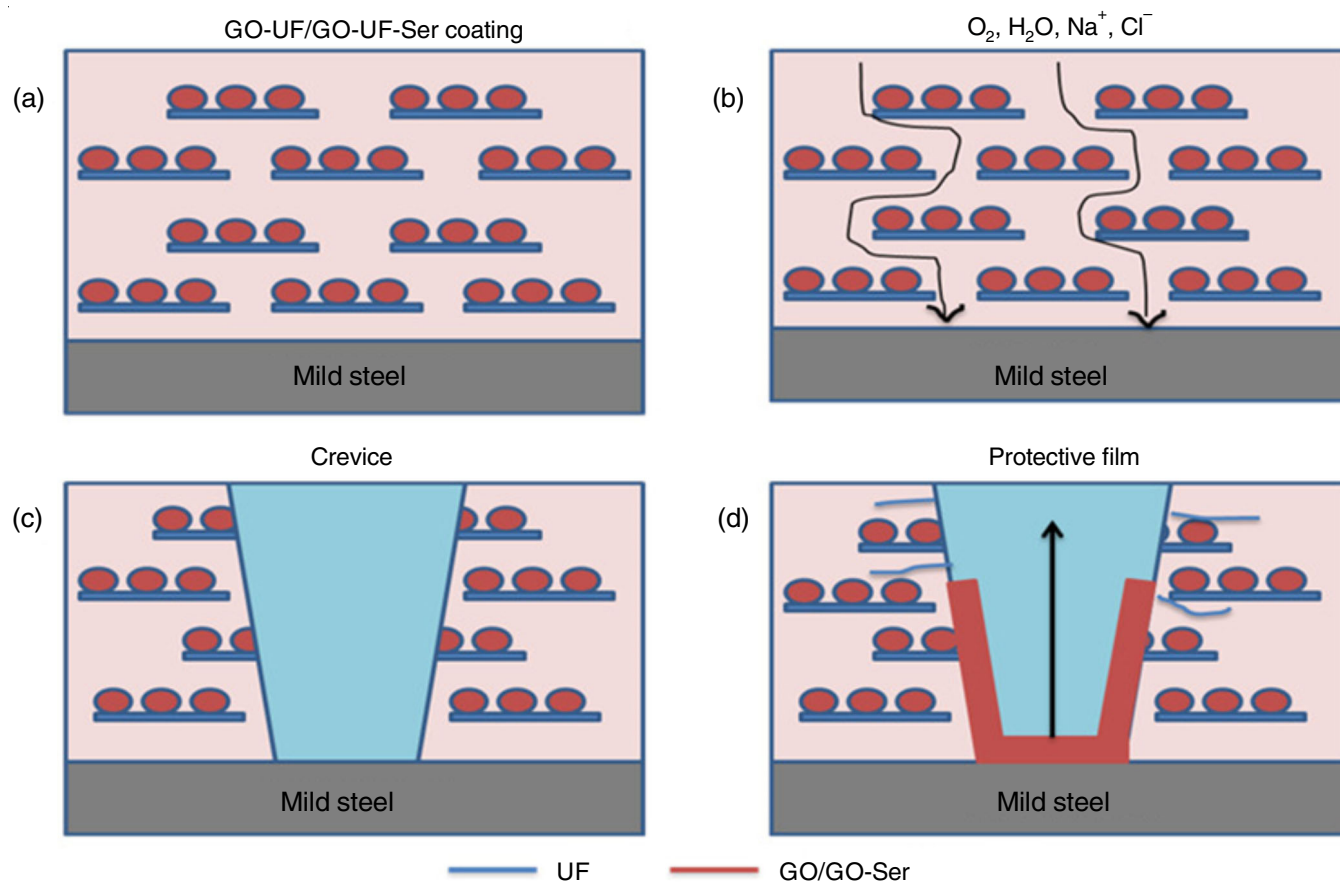


Fig. 15. Diagrammatic portrayal of (a) GO-MC/GO-MC-Ser coatings (b) attack of corrosive ions (c,d) blockade activity of MC-GO/MC-GO-Ser on mild steel surface

## Conclusion

In present work, a promising anti-corrosion coating micro-encapsulated material is developed with enhanced adhesion strength on the steel surface. Initially, the graphene oxide is grafted by serine moiety through the condensation reaction which resulted in the raise of corrosion inhibition performance. Lateron, the serine grafted graphene oxide was further encapsulated in the urea-formaldehyde microcapsules. The MC-GO-Ser microcapsules showed enhanced corrosion resistivity than the other samples. Through the formation of -N-H and -Fe-O linkages, MC-GO-Ser loaded epoxy system established well-built interaction with the mild steel surface. The movement of  $\text{Na}^+$  ions to the cathodic regions was inhibited by this cross-linkage. The overall results revealed that MC-GO-Ser microcapsules tailored in an epoxy matrix demonstrated better corrosion protection and excellent adhesive strength.

## ACKNOWLEDGEMENTS

The authors thank PSGR Krishnammal College for Women for the financial support.

## CONFLICT OF INTEREST

The authors declare that there is no conflict of interests regarding the publication of this article.

## REFERENCES

1. S. Zhou, Y. Wu, W. Zhao, J. Yu, F. Jiang, Y. Wu and L. Ma, *Mater. Des.*, **169**, 107694 (2019); <https://doi.org/10.1016/j.matdes.2019.107694>
2. L.M. Calado, M.G. Taryba, M.J. Carmezim and M.F. Montemor, *Corros. Sci.*, **142**, 12 (2018); <https://doi.org/10.1016/j.corsci.2018.06.013>
3. S.R. Nayak and K.N.S. Mohana, *Surf. Interfaces*, **11**, 63 (2018); <https://doi.org/10.1016/j.surfin.2018.03.002>
4. M.J. Palimi, M. Rostami, M. Mahdavian and B. Ramezanzadeh, *J. Coat. Technol. Res.*, **12**, 277 (2015); <https://doi.org/10.1007/s11998-014-9631-6>
5. B.E. Rani and A. Basu, *Int. J. Corros.*, **2012**, 1 (2012); <https://doi.org/10.1155/2012/380217>
6. D. Wang and G.P. Bierwagen, *Prog. Org. Coat.*, **64**, 327 (2009); <https://doi.org/10.1016/j.porgcoat.2008.08.010>
7. M.G. Sari, M. Shamsiiri and B. Ramezanzadeh, *Corros. Sci.*, **129**, 38 (2017); <https://doi.org/10.1016/j.corsci.2017.09.024>
8. S.E. Karekar, U.D. Bagale, S.H. Sonawane, B.A. Bhanvase and D.V. Pinjari, *Compos. Interfaces*, **25**, 85 (2018); <https://doi.org/10.1080/09276440.2018.1439631>
9. J.E. Gray and B. Luan, *J. Alloys Compd.*, **336**, 88 (2002); [https://doi.org/10.1016/S0925-8388\(01\)01899-0](https://doi.org/10.1016/S0925-8388(01)01899-0)
10. S. Liu, L. Gu, H. Zhao, J. Chen and J. Yu, *J. Mater. Sci. Technol.*, **32**, 425 (2016); <https://doi.org/10.1016/j.jmst.2015.12.017>
11. S. Pourhashem, M.R. Vaezi, A. Rashidi and M.R. Bagherzadeh, *Prog. Org. Coat.*, **111**, 47 (2017); <https://doi.org/10.1016/j.porgcoat.2017.05.008>
12. F. Zhang, P. Ju, M. Pan, D. Zhang, Y. Huang, G. Li and X. Li, *Corros. Sci.*, **144**, 74 (2018); <https://doi.org/10.1016/j.corsci.2018.08.005>

13. G. Kordas, *Corros. Mater. Degrad.*, **3**, 376 (2022); <https://doi.org/10.3390/cmd3030023>
14. L. Liu and J. Xu, *Vacuum*, **85**, 687 (2011); <https://doi.org/10.1016/j.vacuum.2010.10.009>
15. S.S. Golru, M. Attar and B. Ramezanzadeh, *Prog. Org. Coat.*, **77**, 1391 (2014); <https://doi.org/10.1016/j.porgcoat.2014.04.017>
16. Z. Yu, H. Di, Y. Ma, L. Lv, Y. Pan, C. Zhang and Y. He, *Appl. Surf. Sci.*, **351**, 986 (2015); <https://doi.org/10.1016/j.apsusc.2015.06.026>
17. M. Kasaeian, E. Ghasemi, B. Ramezanzadeh and M. Mahdavian, *J. Ind. Eng. Chem.*, **73**, 162 (2019); <https://doi.org/10.1016/j.jiec.2019.01.019>
18. J. Chen, B. Yao, C. Li and G. Shi, *Carbon*, **64**, 225 (2013); <https://doi.org/10.1016/j.carbon.2013.07.055>
19. N.I. Zaaba, K.L. Foo, U. Hashim, S.J. Tan, W. Liu and C.H. Voon, *Procedia Eng.*, **184**, 469 (2017); <https://doi.org/10.1016/j.proeng.2017.04.118>
20. D.C. Marcano, D.V. Kosynkin, J.M. Berlin, A. Sinitskii, Z. Sun, L.B. Alemany, A. Slesarev, W. Lu and J.M. Tour, *ACS Nano*, **4**, 4806 (2010); <https://doi.org/10.1021/nn1006368>
21. L. Shahriary and A.A. Athawale, *Int. J. Renew. Energy Environ. Eng.*, **2**, 58 (2014).
22. A.S. Hicyilmaz and A.C. Bedeloglu, *Mater. Sci. Res. India*, **16**, 07 (2019); <https://doi.org/10.13005/msri/160103>
23. B. Qian, J. Ren, Z. Song and Y. Zhou, *J. Mater. Sci.*, **53**, 14204 (2018); <https://doi.org/10.1007/s10853-018-2615-7>
24. N. Parhizkar, T. Shahrabi and B. Ramezanzadeh, *Corros. Sci.*, **123**, 55 (2017); <https://doi.org/10.1016/j.corsci.2017.04.011>
25. M.S. Eluyemi, M.A. Eleruja, A.V. Adedéji, B. Olofinjana, O. Fasakin, O.O. Akinwunmi, O. O. Ilori, A.T. Famojuro, S.A. Ayinde and E.O.B. Ajayi, *Graphene*, **5**, 143 (2016); <https://doi.org/10.4236/graphene.2016.53012>
26. J. Li, J. Cui, J. Yang, Y. Ma, H. Qiu and J. Yang, *Prog. Org. Coat.*, **99**, 443 (2016); <https://doi.org/10.1016/j.porgcoat.2016.07.008>
27. D. Li and A.W. Neumann, *J. Colloid Interf. Sci.*, **137**, 304 (1990); [https://doi.org/10.1016/0021-9797\(90\)90067-X](https://doi.org/10.1016/0021-9797(90)90067-X)
28. Y. Zhang, D.W. Hazelton, A.R. Knoll, J.M. Duval, P. Brownsey, S. Repnoy, S. Soloveichik, A. Sundaram, R.B. McClure, G. Majkic and V. Selvamanickam, *Physica C*, **473**, 41 (2012); <https://doi.org/10.1016/j.physc.2011.11.013>
29. M. Fadil, D.S. Chauhan and M.A. Quraishi, *Russ. J. Appl. Chem.*, **91**, 1721 (2018); <https://doi.org/10.1134/S107042721810021X>